The Influence of Load Ratio, Temperature, Orientation and Hold Time on Fatigue Crack Growth of CMSX-4

Steffen Müller*, Joachim Rösler, Christoph Sommer* and Walter Hartnagel*
Technical University Braunschweig, Institut für Werkstoffe, Germany
*ABB ALSTOM POWER Technology Ltd., Heidelberg, Germany

ABSTRACT

CMSX-4 is a widely used single crystal material for critical components like gas turbine 1st stage blades and vanes. For lifetime prediction of such components knowledge on defect behavior is of particular interest. For that reason, results of a systematic study, characterizing the influence of load ratio (R=0.1/0.7), temperature (T=550°C/950°C), orientation (<001> and <011> parallel to load axis) and hold times on fatigue crack growth rates will be presented in this paper. It was found, that increasing R and decreasing temperature leads to a reduction of the threshold value for fatigue crack propagation, whereas the fatigue crack growth rate in the Paris region seems to be weekly temperature- and R-dependent. Changing the load axis from <001> to <011> did not influence the fatigue crack growth rate. Independent of temperature, R and loading direction a smooth mode I fracture was found. Room temperature precracking lead to fatigue crack growth along {111} planes. Introducing hold times during fatigue crack growth at 950°C retards the crack propagation rates only at higher stress intensity levels which is attributed to creep deformation during hold times.

Additionally to fatigue crack propagation, isothermal low cycle fatigue (LCF) as well as out-of-phase thermomechanical fatigue (OP-TMF) tests have been performed on test bars with idealized casting defects acting as crack starters. OP-TMF tests compare well with LCF results with compressive dwell time at maximum temperature of TMF tests. LCF tests without dwell time and at lower TMF temperature lead to longer lifetimes. By in-situ observation of crack propagation starting from these defects da/dN data were obtained and compared to those obtained from standard CT specimen. Both for 550 and 950°C, a good agreement between crack growth rates in LCF tests without dwell times and CT results was found.

Superalloys 2000
Edited by T.M. Pollock, R.D. Kissinger, R.R. Bowman,
K.A. Green, M. McLean, S. Olson, and J.J. Schirra
TMS (The Minerals, Metals & Materials Society), 2000

INTRODUCTION

Single crystal (SC) superalloys are widely used for blade and vane applications in aeroengines and, more recently, in land based gas turbines. They offer improved creep and fatigue resistance compared to conventionally and directionally solidified materials due to the lack of grain boundaries, elimination of low melting point elements and anisotropy of elastic modulus. Within the family of SC superalloys, CMSX-4 is a widely used second generation, rhenium containing alloy [1].

For lifetime prediction of SC components such as 1st stage blades and vanes, knowledge on defect behavior, especially under fatigue loading, is of particular interest. Therefore, this article deals with measurement of CMSX-4 fatigue crack growth (FCG) resistance. As systematic studies, characterizing the influence of load ratio, temperature, SC orientation and hold time on FCG, are not available in the open literature for this material, da/dN measurements on standard CT specimen were conducted in <001> and <011> loading direction at two temperatures (550°C, 950°C) and R-ratios (R=0.1, 0.7). By introducing a hold time at the peak stress of the fatigue cycle (300 sec after every 1000 cycles), the influence of creep and/or oxidation effects was determined. Furthermore, low cycle fatigue (LCF) tests at 550°C and 950°C as well as out-of-phase thermomechanical fatigue (TMF) tests (temperature range 550-950°C) have been performed on test bars with idealized casting defects acting as crack starters. These defects, realized with ceramic inclusions with a defined geometry and orientation to the load axis, should give information about the influence of defects in SC material on LCF and TMF lifetime. Besides the characterization of fatigue life of CMSX-4 with and without defects, also fatigue crack propagation has been measured in these tests by means of continuous video monitoring.

EXPERIMENTS

The material used for all tests was taken from a single melt (chemical composition see Table I). From that melt near-net-shape rods or plates were grown by grain selector technique at Doncasters Precision Castings-Bochum GmbH (DPC), Germany. From these ingots, specimens were machined out for the <001> direction parallel to the solidification direction and for <011> direction tilted by 45° to solidification. In both cases <010> was the crack propagation direction. FCG tests were performed at two different laboratories: ABB ALSTOM POWER Ltd. Baden, Switzerland (named AA) and Technical University Braunschweig, Institut für Werkstoffe, Germany (named TUBS). Two different specimen geometries were used: ¾" CT standard specimen at TUBS (thickness ¾") and 1" CT standard specimen at AA (thickness ½") according to ASTM E-647. The crack propagation was monitored continuously by means of potential drop technique in both laboratories. The measured potential signal was converted to crack lengths with Johnson's formula (see ASTM-E647). Whereas the tests at TUBS were performed with a fixed frequency of 5 Hz, the test frequencies at AA ranged from 5 (at high ΔK) to 50 Hz (at low ΔK) within one test. The specimens were heated with a chamber furnace as well as with HF conduction heating.

Table I: Nominal chemical composition of CMSX-4 (in wt.-%, Ni bal.).

Al	Ti	Ta	Cr	Re
5.6	1.0	6.5	6.5	3.0
Mo	**W**	**Co**	**Hf**	
0.6	6.0	9.0	0.1	

TMF and LCF tests were carried on closed-loop servohydraulic testing machines which were equipped with induction heating. Out of the near-net-shape rods cast by DPC cylindrical specimens (diameter 10 mm, gauge length 15 mm) were machined. Loading direction was <001>. The specimens contained rectangular ceramic pins (cross section 1 x 1 mm) in the center of the gauge length, c.p. Fig. 1. The pins have been introduced during the near-net-shape casting process. They penetrated 1 to 4 mm from the surface into the specimens.

LCF tests were performed according to ASTM E 606 under total strain control with a constant strain rate of 6 %/min. Temperature was controlled by a ribbon-like Pt-PtRh thermocouple within the gauge length (see Fig. 1). Testing temperatures were 550°C and 950°C with R = -1. Part of the LCF tests at 950°C included compressive dwell periods of two minutes. The temperature range in the out-of-phase TMF tests was 550°C to 950°C with 2 min compressive dwell times at maximum temperature. The TMF tests have been performed with temperature rates of 3 K/sec and constant mechanical strain rates. Mechanical strain ranges were 0.6 to 0.8%. The number of cycles to crack initiation in the LCF tests was determined at a decrease of the tensile stress amplitude by 5 %. For the evaluation of the TMF tests a 5 % decrease of the maximum tensile stress was used.

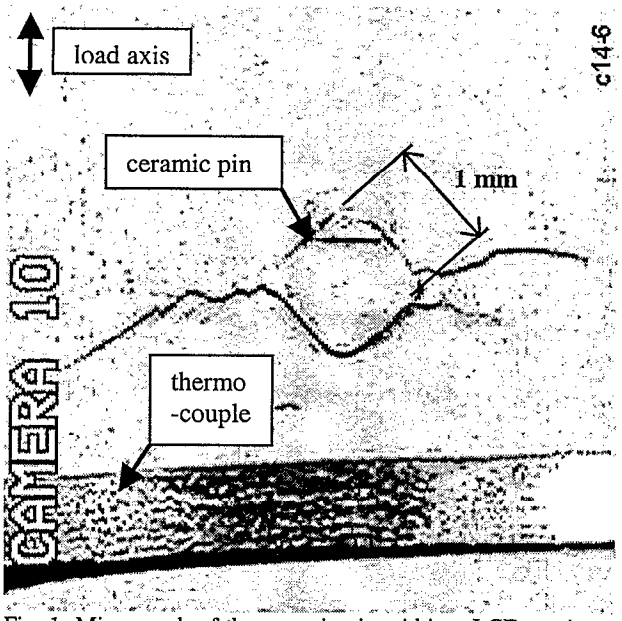

Fig. 1: Micrograph of the ceramic pin within a LCF specimen at 950°C. The picture was taken during testing with the video monitoring system.

The ceramic pins, c.p. Fig. 1, which acted as crack starters were monitored by video observation. After fixed numbers of cycles pictures were stored at maximum strain in the LCF tests and at minimum temperature in the TMF tests. Crack length vs. cycle number data were smoothened by a second order polynom and evaluated crack growth rates compared to fracture mechanics data. According to [2] stress intensities were calculated by

$$\Delta K_I = Y \cdot \Delta\sigma \cdot \sqrt{\pi \cdot a} \qquad (1)$$

with

$$Y = \sqrt{\frac{d+a}{a}}. \qquad (2)$$

$\Delta\sigma$ means tensile stress of the LCF and TMF test, a denotes crack length (measured from pin edge to crack tip) and d denotes half pin width.

RESULTS

Fatigue Crack Growth at 950°C

The fatigue crack growth rates of CMSX-4, loaded in <001> direction, for R ratios of 0.1 and 0.7 are shown in Fig. 2 and 3, respectively. The curves show the typical form with a threshold region and the Paris regime of stable fatigue crack growth. The data for R=0.1 compare well with previous results for CMSX-4 [3] and René-N4 [4]. In agreement with literature findings [5,6], increasing the R-value increases the fatigue crack growth rate for a given ΔK. According to ASTM-E647 the threshold values ΔK_{th} for fatigue crack propagation were determined. The results are summarized in Table II. An increase of R from 0.1 to 0.7 decreases the threshold value for fatigue crack growth by 40%, whereas the FCG rate is accelerated by a factor of about 5 in the Paris regime.

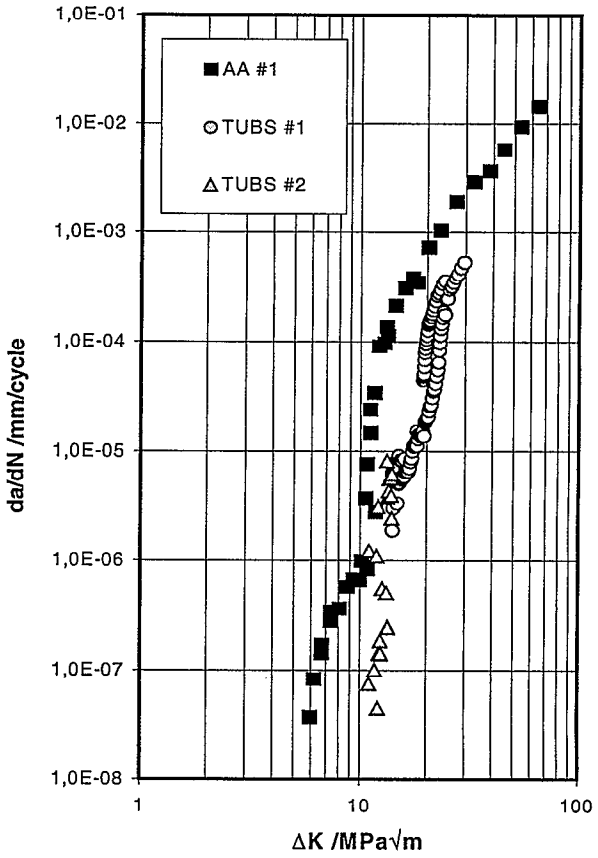

Fig. 2: Fatigue crack growth rates of CMSX-4 at 950°C, <001> load direction and R=0.1 (AA and TUBS refers to test laboratory).

Table II: Threshold values for fatigue crack growth in CMSX-4 at 950°C. For details see text.

T	R=0.1	R=0.7
950	11.0 MPa√m/ 5.5 MPa√m	6.8 MPa√m

Whereas the results for R=0.7 are in a narrow scatter band in the lower stress intensity region (Fig. 3), a strong difference between single measurements for R=0.1 are visible (Fig. 2). One test resulted in a tail at very small ΔK values which predicts a threshold value below 6 MPa√m (compared to 11.0 MPa√m). An explanation for that may be the different test frequencies for the different curves: The tail part of the test named AA was run at frequencies between 40 and 50 Hz,

whereas the curves named TUBS were obtained at a much lower test frequency (5 Hz). At lower test frequencies much more time is spent for oxidation at the crack tip. This oxidation results in crack tip blunting, decreases the stress intensity ahead of the crack tip and leads to a shift of ΔK_{th} to higher ΔK-values [7].

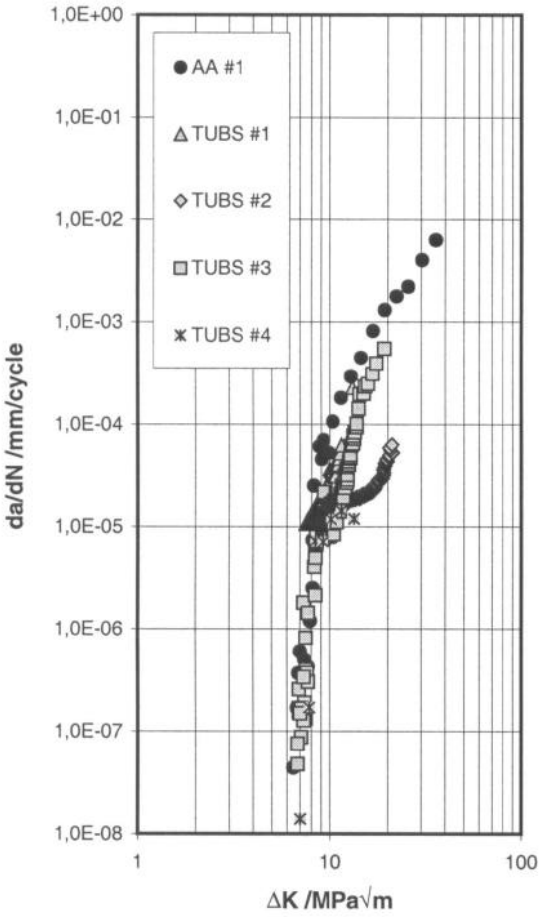

Fig. 3: Fatigue crack growth rates for CMSX-4 at 950°C, <001> load direction and R=0.7 (AA and TUBS refers to test laboratory).

Fractographic investigations of the samples tested at 950°C revealed a macroscopic and microscopic smooth fracture surface (mode I) independent of cyclic stress intensity factor (Fig. 4). This behavior is well-documented in the literature and attributed to the plastic deformation along {100}-planes [8,9]. It is assumed that the homogenous deformation is performed within the narrow γ matrix channels between γ' particles. Additionally, an oxide scale is visible which is probably Al_2O_3 [10]. The thickness of this scale varies only with exhibition time to high temperatures. No influence of stress intensity level or load ratio was found.

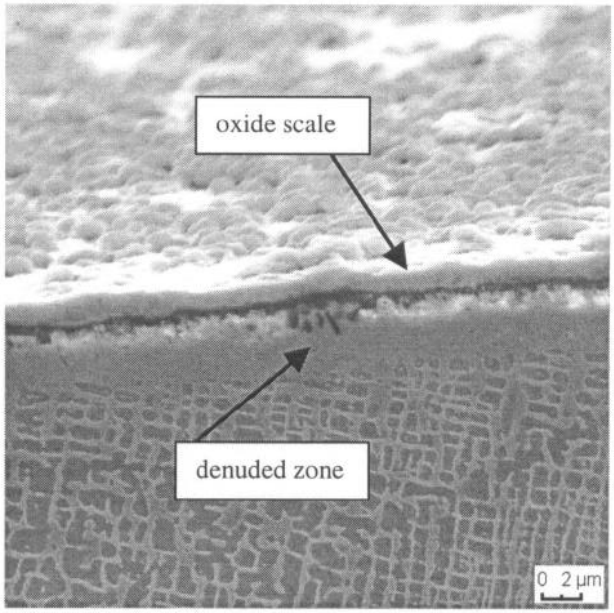

Fig. 4: Fracture path of fatigue crack at medium ΔK at 950°C (R=0.1). A smooth fracture surface with an oxide scale and the γ' denuded zone is visible.

In contrast to high temperature fatigue cracking, fatigue precracking at room temperature leads to crystallographic crack propagation along {111} planes (Fig. 5). These planes are glide planes for CMSX-4 at lower temperatures with the highest shear stresses when the crystal is loaded in <001> direction [3]. This type of fracture was independent of R-value.

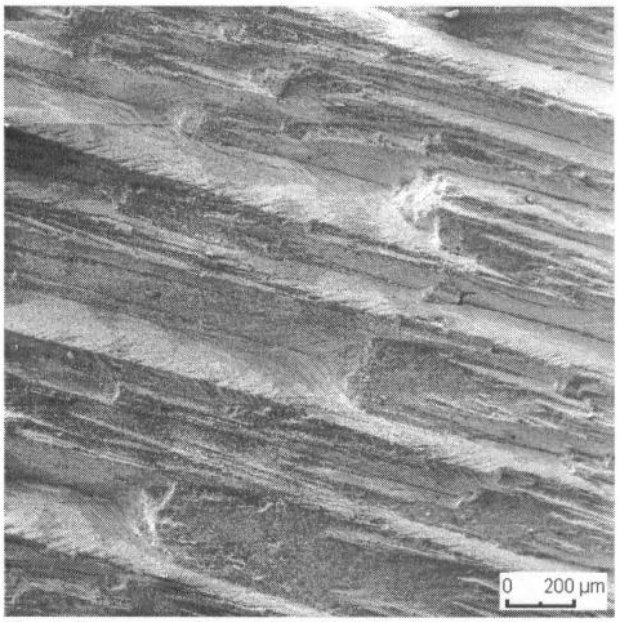

Fig. 5: Fracture surface of CMSX-4 after fatigue crack growth at room temperature (during precracking). A crystallographic fracture along {111} planes is visible.

Fatigue Crack Growth at 550°C

The fatigue crack growth rates for CMSX-4 at 550°C for both load ratios tested (R=0.1 and 0.7) are shown in Fig. 6. Compared with the results for 950°C (Fig. 2 and 3) the following differences were found:

- Surprisingly, testing at 550°C results in smaller threshold values for fatigue crack growth (see Table III) than at 950°C (Table II). This contrasts literature findings where with decreasing temperatures increasing threshold values for fatigue crack growth were found [3,10]. An explanation may be seen in the less intensive oxidation at 550°C. Whereas the growing oxide scale is filling the crack tip and thus, reducing the effective stress intensity factor at 950°C, this mechanism is not possible to act at lower temperatures [11].
- Whereas the Paris region seems to be independent of R, strong differences occur in the threshold region: For both load ratios tested a very strong dependence of the fatigue crack growth rate on the ΔK-value was found. This means, that small changes in the cyclic stress intensity factor leads either to fatigue crack propagation above 10^{-6} mm/cycle or no crack propagation was observed even after 10^6 cycles. Thus, fatigue crack growth rates below 10^{-6} mm/cycle were hardly measurable. This "sharp" threshold at 550°C contrasts the finding of a "smooth" threshold behavior at 950°C (see Fig. 2 and 3).

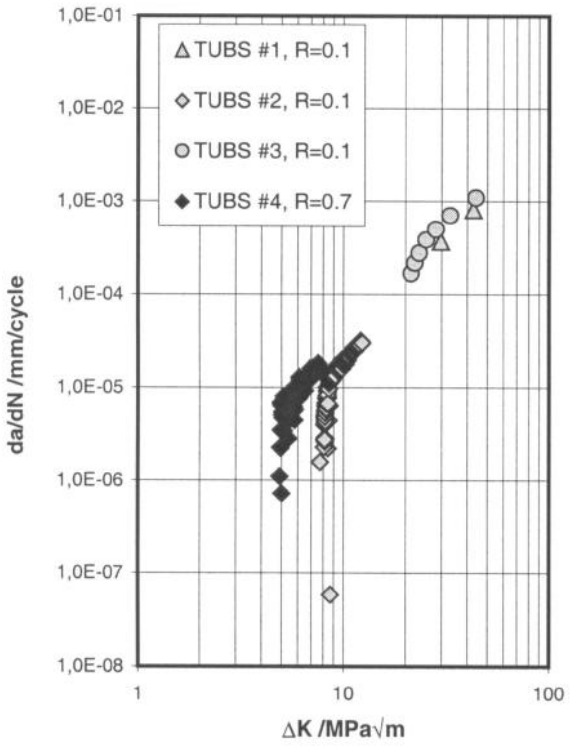

Fig. 6: Fatigue crack growth rates for CMSX-4 at 550°C, <001> load direction, R=0.1 and R=0.7 (TUBS refers to test laboratory).

Table III: Threshold values for fatigue crack growth in CMSX-4 at 550°C.

T	R=0.1	R=0.7
550	8.0 MPa√m	5.0 MPa√m

The fractographic observations made at 550°C were similar to that at 950°C: A macro- and microscopically smooth fracture (mode I on {001} planes) with an oxide scale was found at low and intermediate cyclic stress intensities.

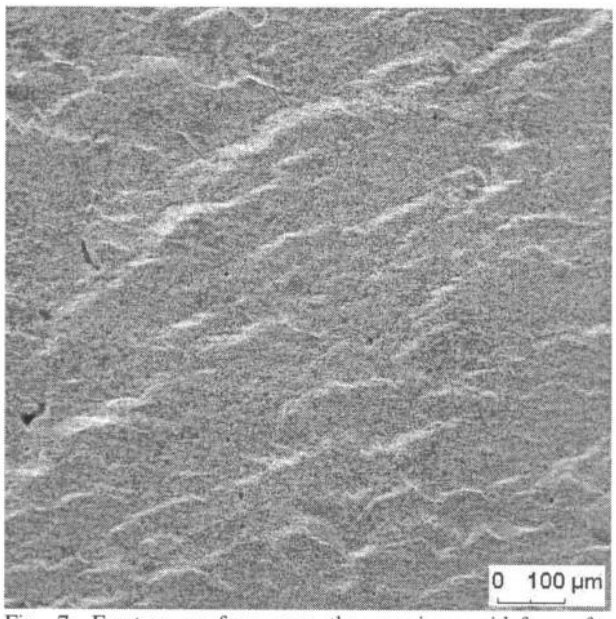

Fig. 7: Fracture surface near the specimen sideface after fatigue crack propagation at higher ΔK and 550°C (R=0.1). A smooth fracture surface with an oxide scale is visible.

At higher cyclic stress intensity factors a deviation from mode I is visible. Especially at the specimen sideface crack propagation along {111} planes was found which could be attributed to the more easily shearing of γ' particles at high stresses [10]. Also a step-wise crack propagation along (macroscopic) {100} and {111} planes was found (Fig. 7).

Influence of Hold Times

In order to study the effect of hold time on fatigue crack propagation, experiments with a hold time at the maximum stress intensity level were performed. Because oxidation and creep effects are expected contributions to fatigue crack growth with hold times, these test were run at 950°C (R=0.7) only. After a package of 1000 cycles (at 5 Hz) a hold time of 300 sec was introduced. The results are given in Fig. 8.

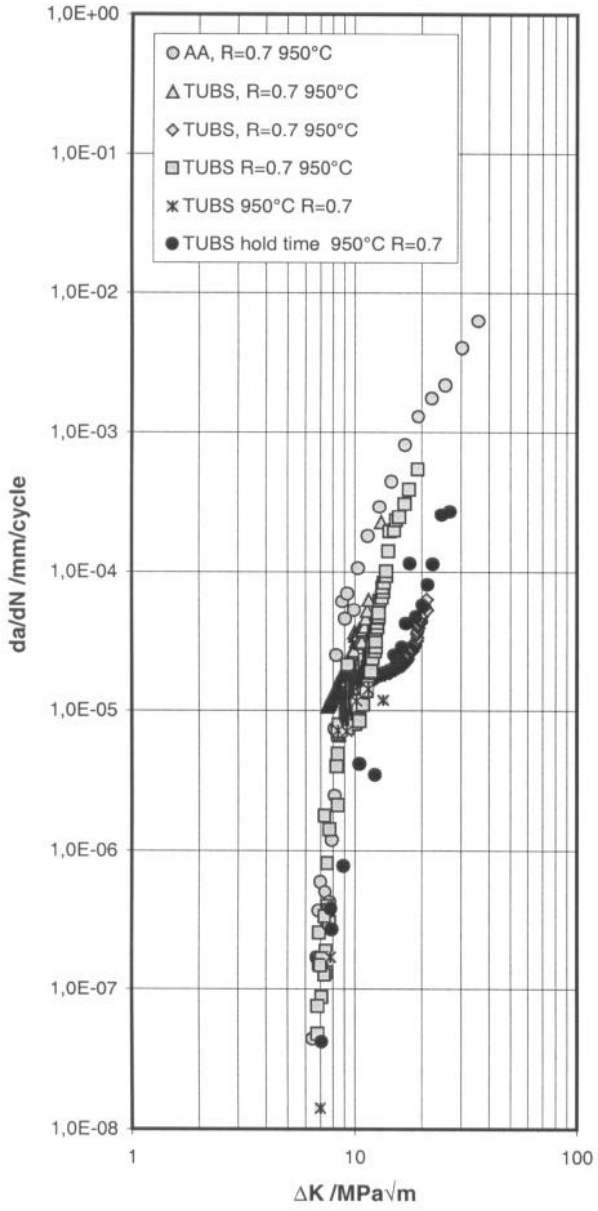

Fig. 8: Influence of hold time on fatigue crack growth rate in CMSX-4 at 950°C (<001> load direction, R=0.7). The hold time of 300 sec was introduced at the peak stress after every 1000 cycles at 5Hz.

As expected from literature findings [12], the introduction of a hold time leads to a retardation of the fatigue crack growth rate by one order of magnitude. But this observation is only true for higher stress intensities. Near the threshold value ($\Delta K<9MPa\sqrt{m}$) no differences between tests with and without hold times were found. In principle, hold time effects may be explained by two contributions: crack tip blunting due to creep deformation and crack closure caused by oxidation. As the oxidation time pre crack growth increment increases with decreasing crack growth rate, the latter mechanism is expected to dominate at low ΔK values. In contrast, crack tip blunting by creep deformation requires sufficiently high stress intensities. Thus, it appears that the observed hold time effect is a consequence of creep deformation rather than oxidation.

The conclusion is also supported by metallographic cross sections of the fracture path after fatigue crack growth with hold times. As shown in Fig. 9 and 10, a wavy structure is apparent where each wave can be a attributed to a hold time. During this hold time, the material creeps and secondary cracks are introduced at higher stress intensities.

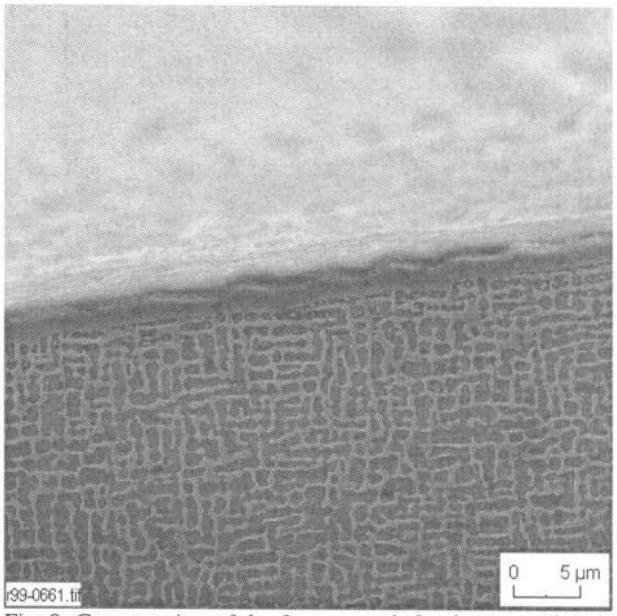

Fig. 9: Cross section of the fracture path for the test with hold times at low ΔK. A wavy structure is apparent.

The above observation is schematically illustrated in Fig. 11. As shown in Fig. 11a, pure fatigue crack propagation is accompanied by a very sharp crack tip. Fig. 11b shows the situation after 300 sec creep hold time: due to creep the crack tip is blunted. This creep time is followed by 1000 pure cycles, leading again to crack tip sharpening and growth (Fig. 11c). The crack length increment is according to the fatigue crack growth rate at the given ΔK level over 1000 cycles. In consequence, a wavy fracture path results where each "step" is associated with hold time creep and the crack advance per fatigue package is given by the distance between "steps".

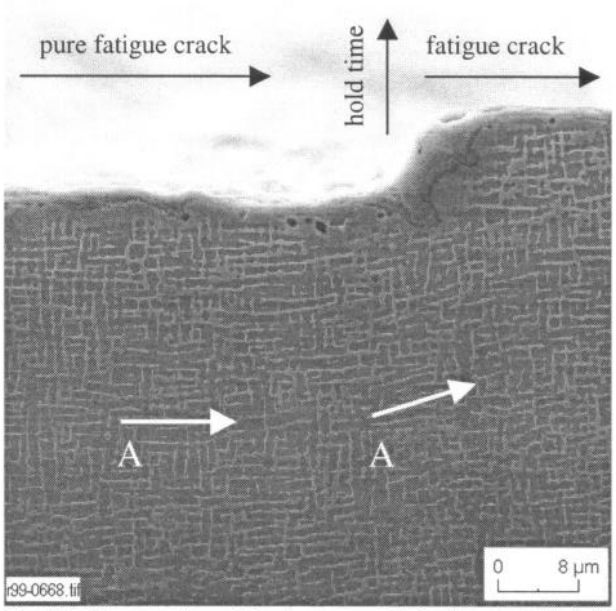

Fig. 10: Cross section of the fracture path for the test with hold times at high ΔK. The wavy structure is clearly visible. The end of each wave is accompanied by creep deformation, which can be seen from deformation of γ' (see arrows A).

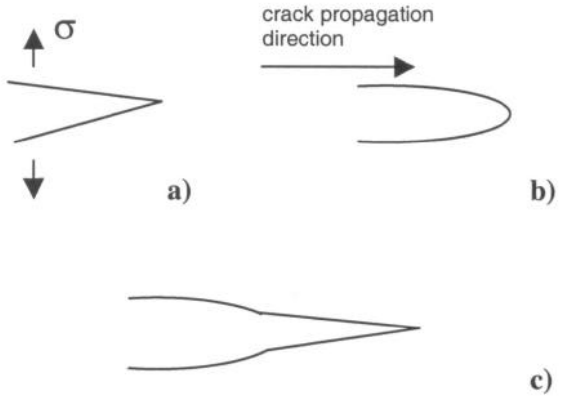

Fig. 11: Schematic illustrating the formation of wavy fracture path during fatigue crack growth with hold times. For details see text.

Influence of Specimen Orientation

No differences between <001> and <011> as loading direction were found at 550°C (R=0.7) as well as at 950°C (R=0.1 and 0.7). All <011> fatigue crack growth curves were in the scatter band of <001> direction with the same curve shape. The fracture surface was again macroscopically smooth and oriented perpendicular to the load axis. The same independence of FCG rates on crystal orientation with respect to load axis was reported for MAR-M200 [13,14].

Low Cycle Fatigue and Thermomechanical Fatigue Tests

In Fig. 12 lifetimes of the TMF tests are compared to those of the LCF tests performed at minimum and maximum temperature. Out-of-phase TMF lives coincided very well with those of LCF dwell time tests at maximum temperature. LCF loading at 950°C without dwell resulted in lifetimes being longer by a factor of approximately 8 while isothermal fatigue at the minimum temperature of the TMF test revealed a further increase of life by a factor of 3 to 4.

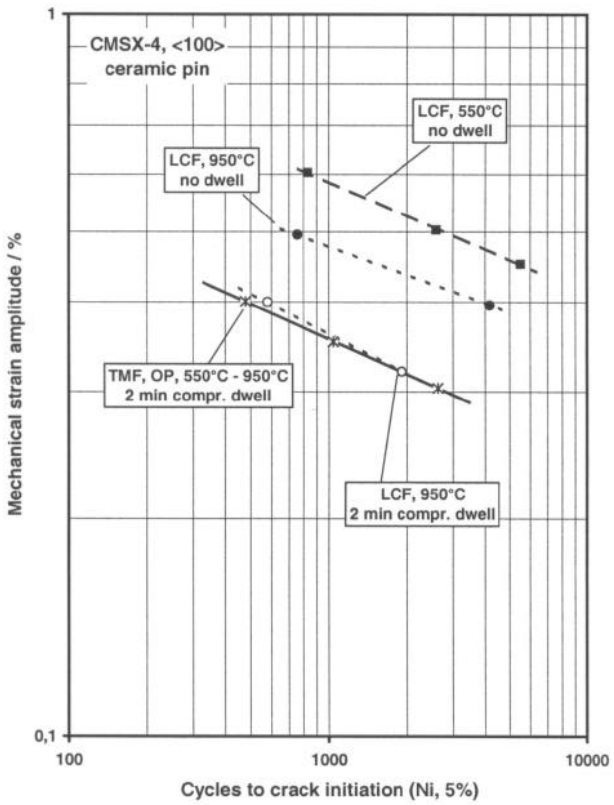

Fig.12: Lifetimes of TMF tests compared with LCF tests performed at minimum and maximum temperature, specimen with ceramic pin as crack starter.

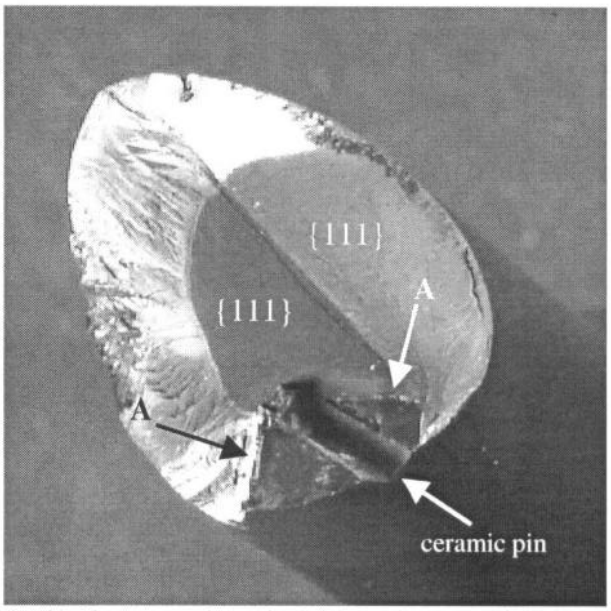

Fig. 13: Fracture surface of a LCF specimen tested at 550°C ($\Delta\varepsilon$=1%, no dwell time, N_f=2600). For details see text.

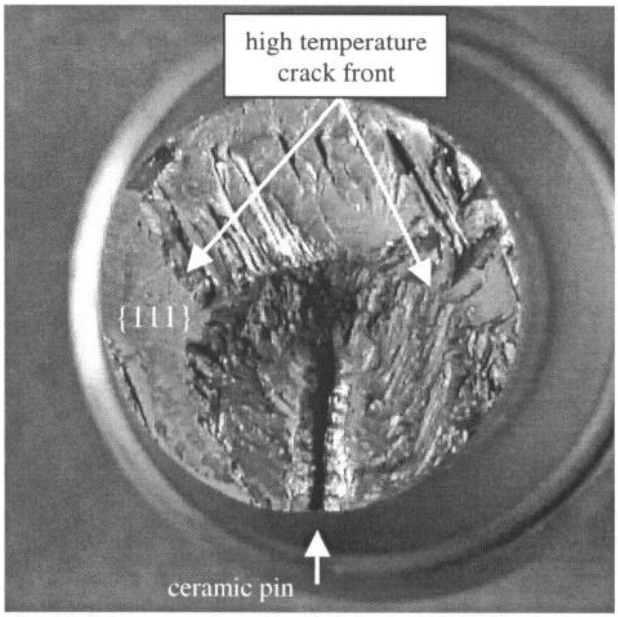

Fig. 14: Fracture surface of a LCF specimen tested at 950°C ($\Delta\varepsilon$=0.8%, 2 min compression dwell time, N_f=720). For details see text.

The fracture surface of a broken LCF sample after testing at 550°C ($\Delta\varepsilon$=1%, no dwell time, N_f=2600) is shown in Fig. 13. Starting from the edges of the ceramic pin the crack propagated macroscopically in Mode I for about 2 mm. This part of fracture, designated with arrows A in Fig. 13, has a smooth surface and is comparable to the fracture type of CT specimen at 550°C. But, as clearly visible in Fig. 13, the crack deviated to grow along two {111} planes. It could be concluded that fracture along {111} is the preferred one because this type, only evident on one side of the ceramic pin, led to complete fracture of the sample. The crystallographic fracture type was never found in CT specimen to such an extend. Only at very high ΔK values some cracking along {111} planes at the surface of the CT specimens was evident which is in agreement with other authors [15]. Probably LCF crack growth rates along {111} planes correspond to very high ΔK values at FCG in CT specimen.

In Fig. 14 the fracture surface of a LCF specimen tested at 950°C ($\Delta\varepsilon$=0.8%, 2 min compression dwell time, N_f=720) is shown. Compared with the tests at 550°C the following features were observed:

- The crack propagates primary at Mode I, but this fracture is accompanied by a microscopically rough fracture surface.
- As at 550°C some crystallographic fracture was observed at 950°C. This type is located at the surface of the sample which may be explained by the plane stress state.

Surface Fatigue Crack Propagation During LCF and TMF Testing

The surface crack length observed at the ceramic pins in dependence on cycle number is plotted in Fig. 15. Comparable crack growth was observed for TMF dwell and LCF dwell at 950°C for comparable strain ranges. Crack growth was reduced for 950°C LCF loading without dwell and lowest crack growth was observed for 550°C LCF tests without dwell. But it must be mentioned, that fast crack growth along {111} planes as shown in Fig. 14 was not included in these crack propagation measurements.

Crack growth rates vs. range of stress intensity (calculated according to Eqn. 1 and 2) are presented in Fig. 16 for the 550°C LCF tests and in Fig. 17 for the 950°C LCF and the TMF tests. Included in both plots are the scatterbands determined by the related CT specimen tests of Fig. 6 and Fig. 2 with the load ratio R = 0.1. For the 550°C tests a good correlation between the standard fracture mechanics fatigue crack propagation test results and the video monitoring of surface crack growth in the LCF tests was observed at high stress intensity ranges. The higher apparent threshold stress intensity ΔK_{th} observed for the LCF tests can be readily interpreted as a consequence of the different R-values. At 950°C LCF crack propagation measured in tests without dwell corresponded well to fracture mechanics data. LCF tests with dwell periods and TMF tests (also with dwell periods) revealed higher crack growth rates. This was attributed to the dwell periods in each cycle which were not included in the fatigue crack propagation tests on standard CT specimens.

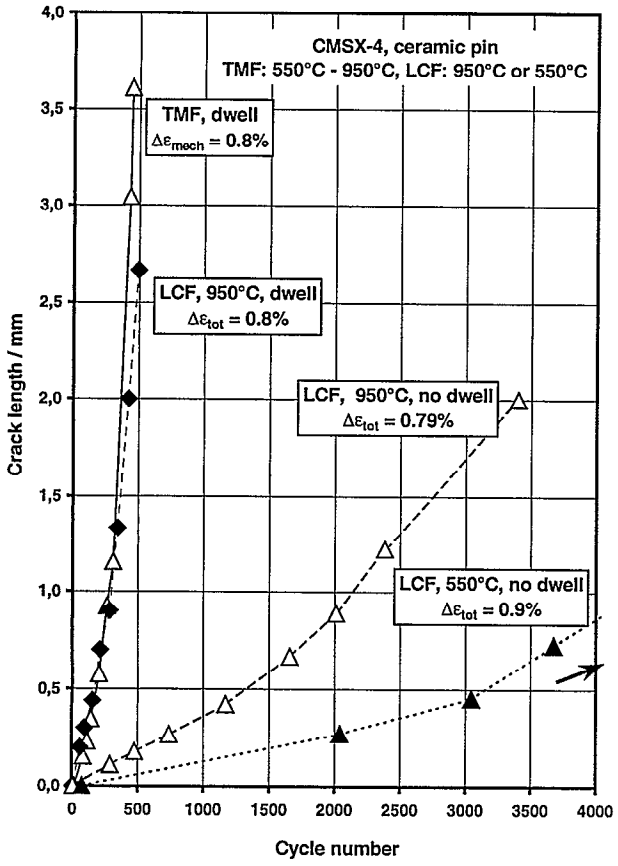

Fig. 15: Crack lengths at the ceramic pins as a function of cycle numbers for TMF tests and LCF tests at minimum and maximum temperature.

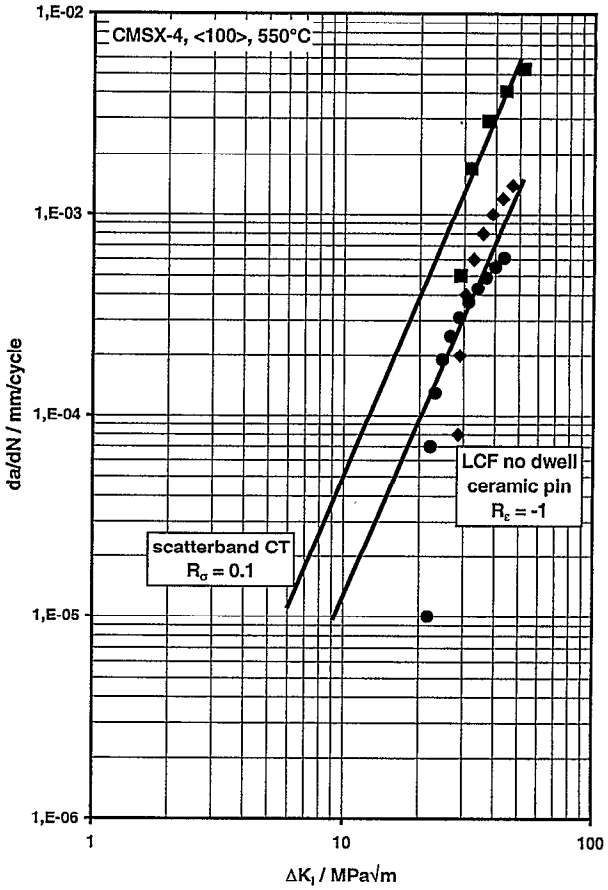

Fig. 16: Crack growth rates vs. range of stress intensity factor for LCF tests at 550°C, LCF specimen with ceramic pin.

CONCLUSIONS

- The fatigue crack growth rate of CMSX-4 in <001> load direction/<010> crack propagation direction showed the following characteristics:
  - Increasing R increases the threshold value ΔK_{th} and the FCG rate in the Paris regime of da/dN at both temperatures.
  - Increasing the temperature from 550°C to 950°C increases the threshold for FCG. Whereas a "sharp" threshold region was found at 550°C, a "smooth" transition from threshold to the Paris regime was found at 950°C.
  - Within the Paris regime, the scatter band of 550°C falls within the band of 950°C data.
- Changing the load axis from <001> to <011> did not influence the FCG rate.
- For all temperatures, R values and orientations a mode I fracture along {001} planes was observed. Room temperature precracking lead to stage I FCG along {111} planes.
- Introducing hold times after 1000-cycle packages during FCG at 950°C/R=0.1, the FCG rate is lowered at higher ΔK due to creep deformation whereas at lower ΔK no influence was found. In contrast, introducing a compressive hold time during LCF/TMF testing reduces the lifetime. Whereas the tensile hold time during FCG leads to creep deformation, the compressive hold time during LCF/TMF testing does not lead to creep, but shifts the mean stress of the cycle to higher tensile stresses.
- In contrast, a compressive dwell time during LCF testing (specimen with ceramic pin) at 950°C leads to a reduction in lifetime by factor 8.
- Out-of-Phase TMF test results compare well with LCF (dwell time at maximum temperature of TMF) data. In contrast, LCF tests at minimum temperature and LCF tests at maximum temperature without dwell time lead to longer lifetimes.
- By comparing the da/dN data from CT specimen with crack propagation starting from defects under LCF/TMF loading the following observations were made:

- At 550°C a good correlation between LCF tests without dwell times and CT results was found.
- At 950°C the LCF data without dwell time fit to data from CT tests, whereas LCF tests with dwell times as well as TMF tests showed higher FCG rates than CT tests. This is somehow surprising since LCF/TMF tests were performed with negative R-values. Probably, short cracks may grow faster than one would expect from long crack growth measurements from CT specimen. This difference seems to manifest itself also in different fracture modes in LCF/TMF and FCG testing.

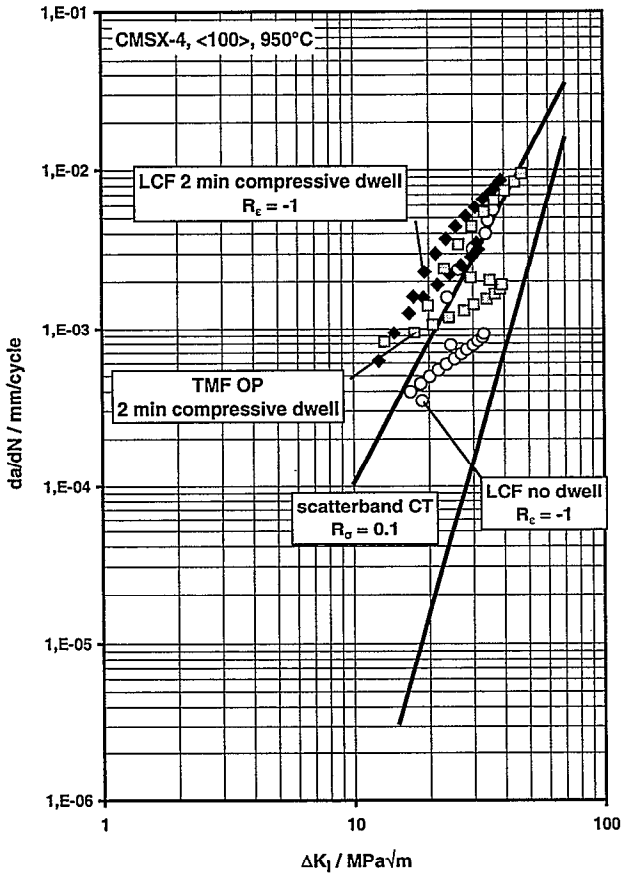

Fig. 17: Crack growth rates vs. range of stress intensity factor for TMF tests and LCF tests at 950°C.

ACKNOWLEDGEMENTS

The work was supported by BMBF grant No. 0327058A and is gratefully acknowledged.

REFERENCES

1. Harries, G.L. Erickson, S.L. Sikkenga, W.D. Brentnal, J.M. Aurrecoechea and K.G. Kubarych, in: Superalloys 1992, S.D. Antolovich et al. (Eds.), 297-306, TMS 1992.
2. O.L. Bowie, J. Math. and Phys., 35, (1956) 60-71.
3. A. Sengupta and S.K. Putatunda, Scripta Met., 31, (1994) 1163-1168.
4. B.A. Lerch and S.D. Antolovich, Met. Trans. A, 21A (1990), 2169-2177.
5. J.S. Crompton, J.W. Martin, Met. Trans. A, 15A (1984) 1711.
6. A. Sengupta, S.K. Putatunda, M. Balogh, J. Mat. Eng. and Perf., 3 (1994) 540-550.
7. E. Affeld, J. Timm, A. Bennet, in: Fatigue under Thermal and Mechanical Loading, J. Bressers et al. (Eds.) 159-169 (Netherlands) Kluwer Academic Publishers 1996.
8. A. Diboine, J. Peltier, R. Pelloux, In: Proc. of MECAMAT Int. Seminar on High Temperature Fracture Mechanisms and Mechanics, Part –IV, P. Bensussan et al. (Eds.), 71-94, Dourdan, France (1987).
9. V. Lupinc, G. Onofrio, G. Vimercati, in: Proc. of the Conf. on Superalloys 1992, S.D. Antolovich et al. (Eds.), 717-726, TMS 1992.
10. T. Rieck, F. Schubert, Berichte des Forschungszentrums Jülich, Nr. 3706, Jülich 1999.
11. M. Henderson, J. Martin, In: Superalloys 1992, S.D. Antolovich et al. (Eds.), 707-716. TMS (1992).
12. G. Onofrio, S. Ai, V. Lupinc, G. Vimercati, Conf.: Fracture Behaviour and Design of Materials and Structures - ECF8, Torino, Italy, 1231-1236.
13. K.S. Chan, J.E. Hack, G.R. Leverant, Met. Trans. A, 18A, (1987) 581-591.
14. K.S. Chan, J.E. Hack, G.R. Leverant, Met. Trans. A, 18A, (1987) 593-602.
15. J. Telesman, L.J. Ghosn, Eng. Frac. Mech., 34, (1996) 1183-1196.